ELSEVIER

Earth and Planetary Science Letters 123 (1994) 155–166

EPSL

Comparison of element and isotope diffusion of K and Ca in multicomponent silicate melts

Sieger van der Laan [1], Youxue Zhang [2], Allen K. Kennedy [3], Peter J. Wyllie

Division of Geological and Planetary Sciences, California Institute of Technology, Pasadena, CA 91125, USA

(Received May 26, 1993; revision accepted March 11, 1994)

Abstract

Recent experimental work has shown that the homogenization of elemental concentrations can be much slower than that of isotopic ratios when there are strong concentration gradients in SiO_2 and Al_2O_3. The ramifications of this result for magma homogenization and other petrological problems related to diffusion are significant. We report here a comparison of experimental profiles of elemental concentrations and isotopic fractions of K and Ca in rhyolite–andesite (large concentration gradients) and rhyolite–rhyolite (small concentration gradients) melt couples.

When the concentration profile and the isotopic profile of the same element in a single couple are compared, the former is much shorter than the latter in the rhyolite–andesite couple, consistent with other recent studies. However, the lengths of both concentration and isotopic profiles are similar in the rhyolite–rhyolite couple. Therefore, diffusion of an element or oxide may be decoupled from or coupled with isotopic 'diffusion', depending on whether large concentration gradients of major components are present.

When the two couples are compared, the intrinsic effective binary diffusivities obtained from isotopic profiles are similar for each element in the two couples, whereas the effective binary diffusivity of K obtained from the concentration profile in the rhyolite–rhyolite couple is 37 times that in the rhyolite–andesite couple. Therefore, isotopic homogenization is roughly independent of elemental homogenization and the presence of SiO_2, Al_2O_3, and other concentration gradients, whereas elemental homogenization is strongly affected by concentration gradients.

Our experimental data (isotopic and concentration profiles including uphill diffusion profiles) can be modeled quantitatively to a good approximation using a modified effective binary diffusion model in which the flux of a component is assumed to be proportional to its activity gradient instead of its concentration gradient. Therefore, the multicomponent diffusion effect in the silicate systems of our experiments seems to be largely due to contributions of non-ideal mixing to the cross-terms of the diffusivity matrix.

1. Introduction

Study of diffusion in multicomponent silicate melts is eventually aimed at allowing us to quantitatively predict the diffusive behavior in complex systems. In principle, diffusion in a multicomponent natural silicate melt can be described by a

[CL]

[1] Mineralogisches Institut, Universität Göttingen, Goldschmidtstrasse 1, 37077 Göttingen, Germany

[2] Department of Geological Sciences, The University of Michigan, Ann Arbor, MI 48109-1063, USA

[3] Department of Applied Physics, Curtin University of Technology, P.O. Box U1987, Perth, Australia 6001

SSDI 0012-821X(94)00051-Y

diffusivity matrix. However, in practice this approach has not been successful [1] due to the lack of adequate data [2]. At present, treatment of diffusion in natural silicate melts is often simplified using an effective binary diffusion model [3], and effective binary diffusivities for each component are determined from experimental data [e.g., 4–8]. However, in multicomponent systems the effective binary approach fails in the case of uphill diffusion (i.e., diffusion of a component against its own concentration gradient). Furthermore, effective binary diffusivities of many components seem to be experiment-specific and to vary with concentration gradients. To alleviate these difficulties, a modified effective binary diffusion model to approximate diffusion in natural silicate melts was recently proposed [1].

Lesher [7] recently carried out experiments to examine the development of both concentration and isotopic profiles. Using a novel experimental approach, Lesher showed that the homogenization of Nd and Sr concentrations can be much slower than that of Nd and Sr isotopic ratios when there is a strong concentration gradient of SiO_2. Lesher's conclusions were also reached by Baker [8], who compared tracer diffusion and trace element diffusion.

The simultaneous monitoring of isotopic and elemental exchange such as that in [7] provides a powerful technique for gaining insights into the diffusion process in a complicated multicomponent system. We report an experimental study expanding upon the study of Lesher [7] in order to compare the concentration and isotopic profiles of major elements, not only when there are large concentration gradients of major components, but also when the concentration gradients of major components are small. In this way the effect of bulk composition and concentration gradients on the development of both the concentration and isotopic profiles can be examined. The experimental data are also modeled using the modified effective binary diffusion model [1].

2. Theoretical background

Diffusive flux of a component i in an N-component silicate melt can be described by [9,10]

$$\boldsymbol{J}_i = -\sum_{j=1}^{N-1} D_{ij}\nabla C_j \tag{1}$$

where the diffusion coefficients (D_{ij}) may depend on the composition and ∇C_j is the concentration gradient of component j. If all gradients are in the same direction (x), ∇C_j reduces to $\partial C_j/\partial x$. Diffusion in a multicomponent system is therefore described by a diffusivity matrix, where there are on-diagonal terms that describe the diffusive flux of a component due to its own concentration gradient and off-diagonal terms that describe the diffusive flux of a component due to concentration gradients of other components. Uphill diffusion of a component (i.e., the diffusion of a component against its own concentration gradient) may occur when the off-diagonal terms contribute more to the flux than the on-diagonal term.

Each element in the diffusivity matrix can be written as [10]

$$D_{ij} = \sum_{k=1}^{N-1} L_{ik}\frac{\partial(\mu_k - \mu_N V_k/V_n)}{\partial C_j} = \sum_{k=1}^{N-1} RTL_{ik}\left(\frac{\partial a_k}{a_k \partial C_j} - \frac{V_k}{V_N}\frac{\partial a_N}{a_N \partial C_j}\right) \tag{2}$$

where L_{ik} represents the phenomenological coefficients that satisfy Onsager's reciprocal relations, R is the gas constant, T is the temperature, and V_k, μ_k, a_k and γ_k are the partial molar volume (assumed to be constant), chemical potential, activity and activity coefficient of component k (similar terms for component N). Clearly elements of the diffusivity matrix contain thermodynamic effects in the form of $\partial a_k/\partial C_j$ [10]. The cross-terms of $\partial a_k/\partial C_j$ are due to the dependence of the activity of component k on the concentration of other components, i.e., due to nonideal mixing. These cross-terms may be particularly large in silicate melts in which complex clusters of ions are expected to be common. It would therefore be desirable to formulate diffusion in terms of activity [1] instead of concentration gradients [1]:

$$\boldsymbol{J}_i = -\sum_{j=1}^{N-1} \mathfrak{D}_{ij}\frac{\nabla a_j}{\gamma_j} \tag{3}$$

where $\mathfrak{D}_{ij}$ is an intrinsic diffusivity. Using activity gradients instead of concentration gradients may reduce the off-diagonal terms and the compositional dependence of the diffusivity matrix.

Because a natural silicate melt contains a large number of components, the diffusivity matrix becomes unmanageably large and an effective binary approach is commonly used [3–8]. For each component i, the effective binary diffusivity D (the subscript i is dropped to simplify notation) is defined as

$$\boldsymbol{J} = -D\nabla C \tag{4}$$

The effective binary diffusivity will be referred to as EBD. The effective binary approach is useful for monotonic profiles, although there are limitations [3]. In the case of uphill diffusion, the EBD as a function of composition is defined but limited in usefulness because its value becomes extremely composition dependent with discontinuities, infinities and negative values along a single profile. By separating thermodynamic effects (i.e., the effect of non-ideal mixing), the compositional dependence of diffusivities may be reduced and the derived diffusion coefficients may be more useful in treating both monotonic and uphill diffusion profiles. Such a modified effective binary diffusion model has been developed [1] based on the idea of transient partitioning of elements in a SiO_2 concentration gradient [11]. This model is summarized below and will be used to treat isotopic and elemental concentration profiles in our diffusion experiments.

In the modified effective binary diffusion model, the diffusive flux of a component is assumed to be proportional to its activity gradient (instead of the concentration gradient as in the conventional effective binary diffusion model):

$$\boldsymbol{J} \approx -\mathfrak{D}\frac{\nabla a}{\gamma} \tag{5}$$

This flux equation is similar to Eq. (4) except that ∇C in the latter is now replaced by $\nabla a/\gamma$. The term $\mathfrak{D}$ in Eq. (5) is the intrinsic effective binary diffusivity (IEBD), which is similar to self diffusivity [1]. The inclusion of γ in Eq. (5) ensures that $\mathfrak{D}$ and D are equal when γ is constant. Note the difference between $\mathfrak{D}$ and D, both in notation and definition. Note that Eq. (5) is an approximation since off-diagonal terms in a $\mathfrak{D}$ matrix are unlikely to be zero [12]. The limitations of the effective binary approach discussed in [3] also apply to the modified effective binary approach [1]. Using Eq. (5), the diffusion equation along one direction is written as

$$\frac{\partial C}{\partial t} = \frac{\partial}{\partial x}\left(\frac{\mathfrak{D}}{\gamma}\frac{\partial(\gamma C)}{\partial x}\right) \tag{6}$$

for component i in an N-component system where $i \neq N$. To estimate γ in Eq. (6), $1/\gamma$ is assumed to be a linear function of $SiO_2 + Al_2O_3$ concentration. Assuming γ to be an exponential function of $SiO_2 + Al_2O_3$ concentration does not make a significant difference [1]. For the justification of this assumption, see discussions in [1] and fig. 4 in [13]. Diffusion of $SiO_2 + Al_2O_3$ is assumed to be approximately effective binary (i.e.,

[1] Some reviewers suggested that the chemical potential and the phenomenological coefficients (L) should be used to formulate the diffusive flux. Using activity gradients is equivalent to using chemical potential gradients except for factors that relate $\mathfrak{D}$ and L and involve the concentrations. Because of the factors associated with concentrations, using activity gradients is superior to using chemical potential gradients (see [10], p. 14–15). The following example helps to illustrate this point: Consider an ideal binary solution where $V_1 = V_2$. When component 1 is present at minor or trace level, $J_1 = -L\partial(\mu_1 - \mu_2)/\partial x \approx -L\partial\mu_1/\partial x$. Using the concentration gradient, $J_1 = -D\partial C_1/\partial x$. The two approaches are equivalent with $D = RTL/C_1$. Consider the following two cases

Case 1: C_1 varies linearly with distance, $C_1 = 10^{-3}$ at $x = 0$ mm, and 10^{-2} at $x = 1$ mm.

Case 2: C_1 varies linearly with distance, $C_1 = 10^{-18}$ at $x = 0$ mm, and 10^{-17} at $x = 1$ mm.

The average chemical potential gradients in both cases are $RT\ln 10$/mm, while the concentration gradient in Case 1 is 10^{15} times that in Case 2. Clearly the diffusive flux in Case 1 must be roughly 10^{15} times that in Case 2 because there are not many atoms of the component in Case 2. So L (the phenomenological coefficient) cannot be constant but must be roughly proportional to the concentration while D (proportional to L/C) is approximately constant. Therefore, using concentration gradients to formulate the diffusive flux is superior to using chemical potential gradients if the mixture is ideal. Similarly, using activity gradients is superior to using chemical potential gradients for non-ideal mixtures.

the concentration is an error function of $x/\sqrt{4D_b t}$ for an infinite-medium diffusion couple, where D_b is the EBD of $SiO_2 + Al_2O_3$). Therefore, $1/\gamma$ as a function of x and t for diffusion in an infinite diffusion couple can be expressed as follows:

$$\frac{1}{\gamma} = 1 + Q \operatorname{erf} \frac{x}{2\sqrt{D_b t}} \tag{7}$$

where Q is a parameter related to the 'partitioning' of the component between the liquids of the left and right halves of the diffusion couple. The interface liquid is assumed to be the standard state with $\gamma = 1$ in Eq. (7). Two-liquid partition coefficient K is related to Q by $K = (1 + Q)/(1 - Q)$. Knowing the $SiO_2 + Al_2O_3$ profile, D_b can be obtained and γ in Eq. (7) can be calculated given x, t and Q. Hence, knowing the initial concentrations of the component (or the isotope) in the two halves, diffusion in an infinite diffusion couple can be calculated from Eqs. (6) and (7) given the two parameters $\mathfrak{D}$ and Q (in conventional effective binary treatment, there is only one parameter, D). Therefore, the model may be used to fit experimental diffusion profiles. The model has been used successfully to fit diffusion profiles generated during crystal dissolution [1]. In this study, we apply the model to isotopic and elemental concentration profiles generated by diffusion couple experiments.

3. Experimental and analytical techniques

Two diffusion couples were prepared for the diffusion experiments. Each couple consists of a natural rhyolitic glass and a synthetic isotopically doped gel (Table 1). One synthetic gel is rhyolitic and the other andesitic, compositionally similar to rocks. The choices of these compositions ensure applicability to natural magma mixing processes. Both gels were spiked with ^{41}K and ^{42}Ca. They were synthesized through precipitation from solution followed by stepwise heating to 900°C to drive off volatiles [14]. The gels consisted of a homogeneous, non-crystalline mixture of oxides with a 3–5% relative perturbation in ^{41}K and ^{42}Ca isotope fractions.

Table 1
Composition of starting materials [a]

wt%	Rhyolite glass	Rhyolite[b] gel	Andesite[b] gel
SiO_2	77.0	72.8	59.0
TiO_2	0.22	0	0
Al_2O_3	12.5	14.5	17.3
FeO	3.18	1.65	7.20
MnO	0.06	0	0
MgO	0.07	.34	3.17
CaO	1.66	1.44	6.74
Na_2O	4.13	3.68	4.12
K_2O	2.75	5.07	1.58
H_2O[c]	0.26	1.22	0.92
Total	101.8	100.7	100.0
$^{41}K/\Sigma K$ %[d]	6.74	6.95	6.98
$^{42}Ca/\Sigma Ca$ %[d]	0.646	0.676	0.666

[a] Microprobe analyses except for H_2O and isotope fractions. [b] Synthetic and isotopically spiked. [c] Total water concentrations in terms of H_2O are determined with a Nicolet 60SX Fourier transform infrared spectrometer at the University of Michigan. Measurements were on glasses after the experiments. The molar absorptivities of Newman et al. [22] for rhyolitic glasses are used to estimate the total water contents in all the samples, which may cause some error for the andesite sample. [d] Isotope fractions have not been corrected for mass fractionation effects as the measured isotope fractions in our natural rhyolite glass deviates only slightly from the natural isotope fractions (6.74 vs. 6.73 for $^{41}K/\Sigma K$, and 0.646 vs. 0.647 for $^{42}Ca/\Sigma Ca$).

A pellet of isotopically spiked rhyolitic or andesitic gel (2.5 mm long and 2 mm in diameter) was tightly pressed into a Pt capsule. Then a rhyolite glass cylinder of similar size with a polished contact surface was pressed into the capsule on top of the gel. The capsules were crimped and then welded at 400°C on a hot stage to minimize trapped volatiles (air and water vapor). The two encapsulated couples were run in a single experiment to avoid differences in experimental conditions. The capsules were enclosed in a graphite disk to minimize temperature gradients and run in a vertical position in a 19.1 mm piston-cylinder apparatus at a nominal pressure of 1.0 GPa (hot piston-in procedure) and 1250°C. CaF_2 was used as the pressure medium. The

temperature was controlled and monitored with a type-S thermocouple. After 30 min the run was quenched to glass roughly isobarically. Concentration profiles across the interface along the approximately 5 mm long couples were measured with a JEOL-733 electron microprobe at Caltech and a CAMECA electron microprobe at the University of Michigan. Isotopic ratio profiles were measured with a CAMECA IMS3F ion microprobe at Caltech. The precision of the analyses

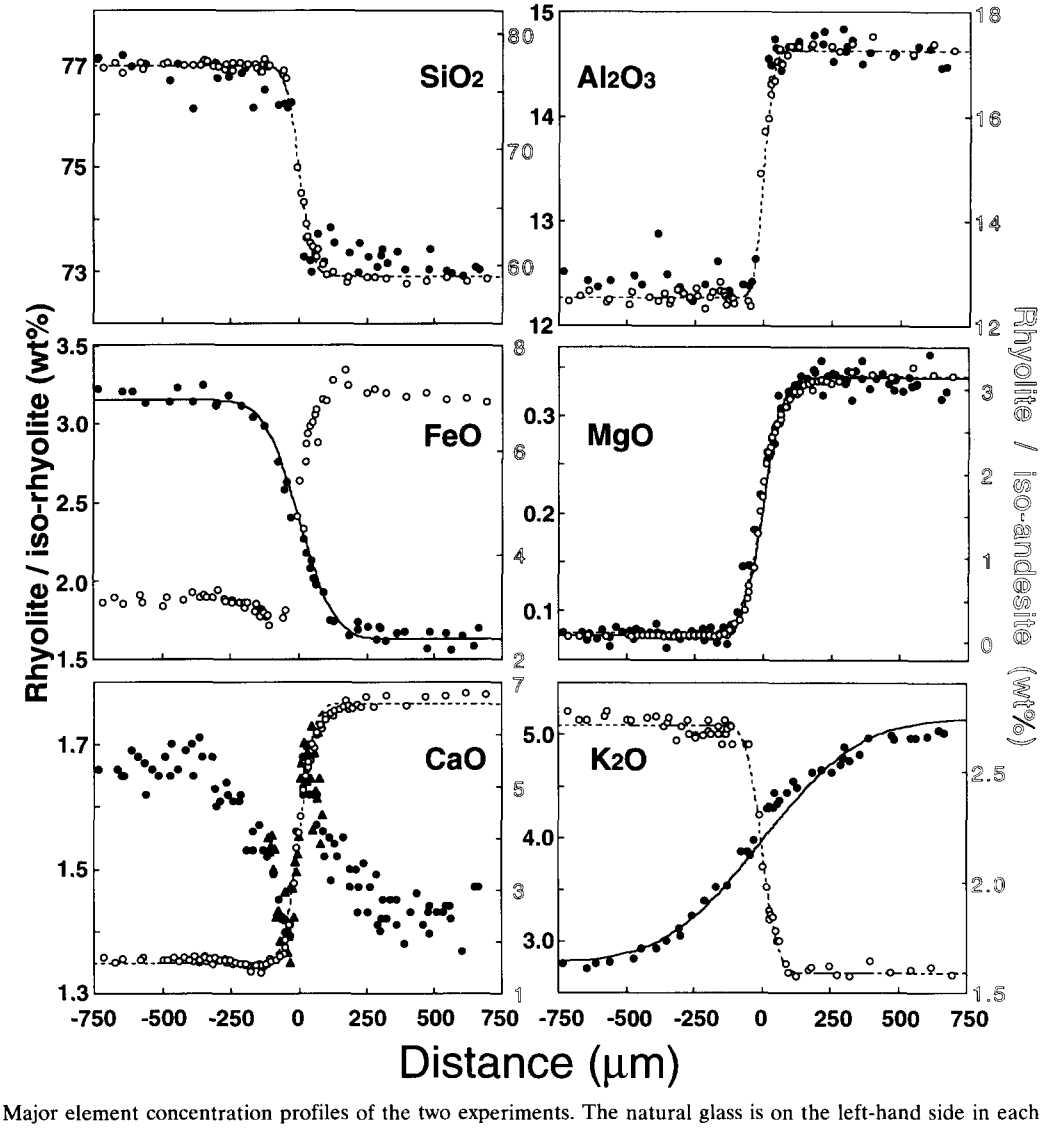

Fig. 1. Major element concentration profiles of the two experiments. The natural glass is on the left-hand side in each figure, and the synthetic and isotopically spiked half is on the right-hand side. Black symbols (data) and solid lines (fits of data by Eq. 8) are for the rhyolite–rhyolite (i.e., rhyolite/iso-rhyolite) couple (143) (scale in boldface on the left-hand vertical axis). Circles (○) (data) and dashed lines (fits of data by Eq. 8) are for the rhyolite–andesite (i.e., rhyolite/iso-andesite) couple (144) (scale in outline-face on the right-hand vertical axis). Black triangles (▲) are CaO analyses from the CAMECA microprobe at the University of Michigan; all other points are JEOL microprobe data acquired at Caltech. The CAMECA microprobe data for CaO were adjusted by multiplying a constant factor of 0.985 so that the concentrations at the ends match (equivalent to running a common standard). Data points outside the −750–750 μm range are not shown in the figures but are used in the fittings.

can be seen from the scatter at the ends and from the smoothness of data points along the profiles.

Convection is unlikely to occur considering the high viscosity of these melts. Possible convection is evaluated by measuring several traverses in each experimental charge. They are identical within error, suggesting that convection in the melt during the experiment was unlikely. The difference in the length of concentration profiles for K_2O, CaO and other elements is consistent with the notion that mass transfer occurred through diffusion rather than convection.

4. Results and discussion

4.1. Major element profiles and effective binary diffusivities

Major oxide concentration profiles of the two experiments are given in Fig. 1. The actual interface of a diffusion couple is not marked in the experiment and is not known. The interface position is obtained so that the fits are optimized. The vertical scales in Fig. 1 are different for the two couples so that the concentrations at the ends plot at similar positions. The scaling helps to compare the lengths of the diffusion profiles in the two couples. The SiO_2, Al_2O_3 and MgO profiles of the two couples are close to identical although the initial concentration differences between the ends are very different in the couples. The profiles of Na_2O (not shown due to low precision) showed uphill diffusion in the couples. The profiles for FeO, CaO and K_2O of the two couples are dissimilar (clearer views of CaO and K_2O profiles are shown in Figs. 2 and 4), not only because the concentration contrasts in the couples are reversed, but also in the shape of the profiles. The profile for FeO shows uphill diffusion in the rhyolite–andesite couple but is monotonic in the rhyolite–rhyolite couple. Both the CaO and K_2O profiles show steep and narrowly confined gradients in the rhyolite–andesite couple but shallower gradients developed over considerable length in the rhyolite–rhyolite couple. In the rhyolite–andesite couple the CaO and K_2O gradients developed over a distance similar to that of SiO_2 and Al_2O_3, and could be interpreted as transient 'equilibrium' partitioning [11].

For monotonic diffusion profiles, we have obtained the EBDs by fitting the profiles to the solution for a diffusion couple with constant D [e.g., 15]:

$$C = \frac{C_1 + C_2}{2} + \frac{C_2 - C_1}{2} \operatorname{erf} \frac{x - x_0}{2\sqrt{Dt}} \tag{8}$$

where C_1 and C_2 are the initial concentrations of the component in the two halves of the couple, and x_0 is the interface position that is varied to optimize the fits. The EBDs with 2σ errors [16] are listed in Table 2. These 2σ errors do not include experimental errors such as errors in temperature, pressure, run duration, charge deformation and diffusion during run-up. (These factors affect both the isotopic and concentration profiles, so comparison of the isotopic and concentration profiles in a diffusion couple is not affected by them.) Since most profiles can be fit well by an error function, the compositional dependence of D is small across the profile. The MgO and CaO profiles for the rhyolite–andesite couple show slight asymmetry, indicating greater diffusivities at the andesite side.

The EBD of K_2O in the rhyolite–rhyolite couple is 37 times that in the rhyolite–andesite couple (Table 2). The large difference in the EBD of K_2O between the two couples cannot be attributed to a compositional difference because (i) the K_2O profile in the rhyolite–andesite couple can be fit by a constant D although there is a large compositional contrast in the couple, and (ii) the rhyolite–andesite couple has a lower average $SiO_2 + Al_2O_3$ concentration than the rhyolite–rhyolite couple and is expected to have a greater D [4,5] yet the observed D is lower. We attribute the large difference in D_K to the difference in the concentration gradients for the two couples. In the context of the modified effective binary diffusion model, it has been shown that the EBD of a component obtained from diffusion profiles depends on the concentration gradients of $SiO_2 + Al_2O_3$ and the component itself [1]. The difference in D_K of the two couples can also be explained using the diffusivity matrix (Eq. 1).

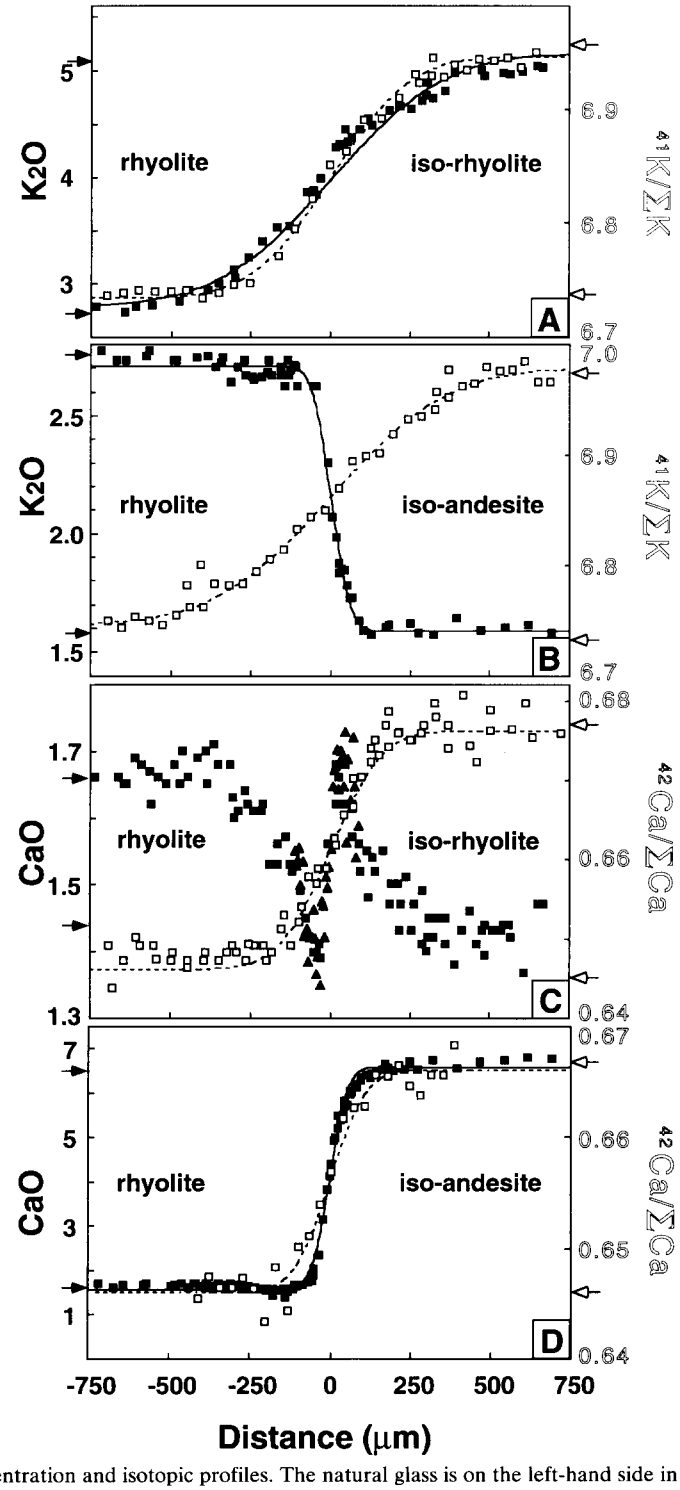

Fig. 2. Comparison of concentration and isotopic profiles. The natural glass is on the left-hand side in each figure, and the synthetic and isotopically spiked half is on the right-hand side. Black symbols (data) and solid lines (fits of data by Eq. 8) refer to oxide concentrations (wt%, scale in boldface on the left-hand vertical axis). White symbols (data) and dashed lines (fits of data by Eq. 8) refer to isotope fractions (%, scale in outline-face on the right-hand vertical axis). Compositions of starting materials are indicated with arrows.

Table 2
Diffusivities from diffusion couple experiments at 1250°C and 1.0 GPa

Experiment	#143 Rhyolite-rhyolite		#144 Rhyolite-andesite	
	D^a $\mu m^2/s$	fitting error[b]	D^a $\mu m^2/s$	fitting error[b] wt%
SiO_2	—	—	0.45±0.07	0.89
Al_2O_3	—	—	0.22±0.05	0.29
FeO	2.9±0.7	0.11	uphill diffusion[c]	
MgO	1.11±0.22	0.02	0.89±0.09	0.15
CaO	uphill diffusion[d]		0.57±0.09	0.34
K_2O	22±5	0.21	0.60±0.14	0.08
	$\mathcal{D}^e$	fitting error[b]	$\mathcal{D}^e$	fitting error[b]
$^{42}Ca/\Sigma Ca$	4.4±1.4	0.005	2.2±1.7	0.003
$^{41}K/\Sigma K$	10.7±2.2	0.014	23±6	0.018

[a] EBDs $\pm 2\sigma$ errors. [b] The 2σ error in terms of the concentration (wt%) of the component to be fit (i.e., the average difference between the calculated and the measured), or in terms of the isotopic fraction (%) to be fit. [c] The uphill diffusion profile was fit to obtain an IEBD of $\sim 13\ \mu m^2/s$ (Fig. 4). [d] The uphill diffusion profile was fit using the IEBD obtained from the $^{42}Ca/\Sigma Ca$ profile (Fig. 4). [e] Diffusivities obtained by fitting isotopic fraction profiles; these diffusivities are similar to IEBDs.

Since concentration gradients are small for components other than K_2O in the rhyolite–rhyolite couple, the contribution to K_2O diffusion from other gradients should be small unless cross coefficients D_{ij} are much larger than the main coefficient (D_{KK}), whereas in the rhyolite–andesite couple the contribution to K_2O diffusion from other gradients is expected to be large. Therefore, a large difference in D_K for the two couples is possible.

The CaO diffusion profile in the rhyolite–andesite couple is monotonic (Fig. 2D) but that in the rhyolite–rhyolite couple shows uphill diffusion (Fig. 2C). The occurrence of uphill diffusion in the latter case is expected due to a small initial CaO concentration gradient. In the context of the modified effective binary diffusion model, uphill diffusion occurs when the activity gradient of the component is opposite to, or greater than the concentration gradient. An almost zero initial concentration difference in the two halves is the most favorable case for the development of uphill diffusion because the activity gradient is unlikely to be zero. Using the multicomponent diffusion argument, an almost zero initial concentration gradient is also the most favorable case to develop uphill diffusion because cross-term contributions due to other gradients easily dominate the diffusive flux of CaO (Eq. 1).

4.2. Isotopic fraction profiles and comparison with concentration profiles

Isotopic ratios are cast into the form of isotopic fractions, $^{41}K/\Sigma K$ and $^{42}Ca/\Sigma Ca$, where ΣK and ΣCa are the summation of all K and Ca isotopes respectively. Fractions are used because it has been shown that the length of a fraction profile reflects the IEBD better than an isotopic ratio profile [1]. The fraction profiles are shown and compared with oxide concentration profiles in Fig. 2. The interface positions for isotopic fractions are in general not at the center of the profile when the initial concentrations of the two halves are not equal [1,7]. For the purpose of obtaining diffusivities and of comparison with oxide concentration profiles, the interface is depicted as at the center in Fig. 2. Profiles of $^{41}K/\Sigma K$ and $^{42}Ca/\Sigma Ca$ are fit by Eq. (8) to derive diffusivities. The isotopic fraction profiles are affected by both isotopic exchange and the diffusion of the elements. Nevertheless, fitting of isotope fraction profiles gives a rough estimate of IEBD [1]. These diffusivities are listed in Table 2 and will be referred to as the IEBD.

The K_2O concentration profile and the $^{41}K/\Sigma K$ profile in the rhyolite–rhyolite couple (Fig. 2A) are almost identical in length, indicating similar EBD and IEBD. On the basis of the fitting results, the EBD of K_2O is slightly greater than the IEBD obtained from the $^{41}K/\Sigma K$ profile. The small difference may not be significant, but if significant it is consistent with the prediction made in fig. 3B of [1]. The lengths of the K_2O concentration and $^{41}K/\Sigma K$ profiles differ significantly in the rhyolite–andesite couple (Fig. 2B), where the IEBD is about 39 times the EBD.

For Ca, the IEBD is about 5 times the EBD in the rhyolite–andesite experiment (Fig. 2D). Calcium in the rhyolite–rhyolite experiment (Fig. 2C) shows uphill diffusion, but the concentration

and isotope gradients developed over similar lengths. Our results for the rhyolite–andesite couple are similar to those of Lesher [7], with smaller EBD than IEBD (decoupling). However, the rhyolite–rhyolite couple that has small compositional contrasts shows a different behavior, with similar lengths of concentration and isotopic profiles (coupling).

Although there is a large compositional difference between the two couples (especially the rhyolite gel half versus the andesite gel half), and although there is a large difference in the EBD of K_2O between the two couples, the IEBDs of K and Ca in the two experiments are similar to each other (within a factor of 2.2). This observation suggests that the IEBDs of K and Ca are not strongly compositionally dependent in the compositional range that we have studied, and neither do they depend strongly on the concentration or activity gradients of other components. The EBD, on the other hand, depends strongly on the concentration gradients of the components (compare D_K in the two couples). All this is consistent with the conclusions in [1]. Therefore, isotopic homogenization is expected to proceed at roughly the same rate independent of concentration gradients [7], while concentration homogenization depends on the concentration gradients.

The IEBDs of Ca from this study are compared with the IEBD and self diffusivities obtained by other authors in Fig. 3. No attempt is made to compare K diffusivities because the only other results of K self diffusion are those of Jambon [17] at much lower temperatures than our experiments. Fig. 3 shows that our $\mathcal{D}_{Ca}$ data on rhyolite and andesite glasses with 0.3–1.2% total water lie between the extrapolated Ca self diffusivities in dry obsidian and a wet obsidian with 6.2% water obtained by Watson [18], suggesting a consistency between the datasets. The Ca self diffusivities of Jambon [17] seem to have too high an activation energy (i.e., too steep a slope in Fig. 3). Our data are also not too far off the IEBDs in basaltic andesite of Zhang [1] and the self diffusivities of Hofmann and Magaritz [19], considering the pressure effect and the compositional effect.

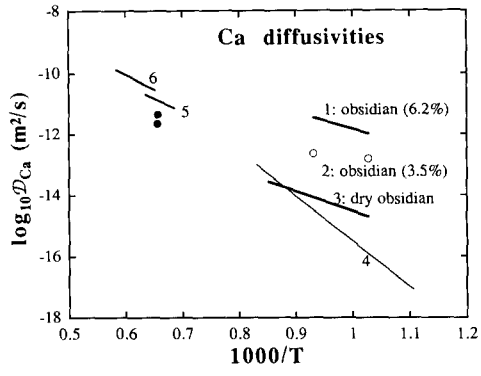

Fig. 3. Available IEBDs and self diffusivities of Ca. Sources of data: ● = this work; line 1, ○ and line 3 = self diffusivities from Fig. 6 of Watson [18] (obsidian with 6.2%, 3.5% and ~ 0.17% water, 2.1 kbar); line 4 = self diffusivities from table 3 of Jambon [17] (obsidian with ~ 0.5% water, 1 bar); line 5 = IEBDs of Zhang [1] (basalt to andesite, 5 kbar); line 6 = self diffusivities of Hofmann and Magaritz [19] (olivine tholeiite, 1 bar).

4.3. Application of the modified effective binary diffusion model

There are several intriguing profiles that have not been treated quantitatively. There is uphill diffusion for CaO in the rhyolite–rhyolite couple and for FeO in the rhyolite–andesite couple. The K_2O concentration profile in the rhyolite–andesite couple is much shorter than the isotopic profile. In this section the modified effective binary diffusion model [1] is used to quantitatively model these profiles.

We first examine these profiles qualitatively using the transient equilibrium partition concept as applied to diffusion by Watson [11]. Two-liquid partition data suggest that at transient 'equilibrium' CaO would be enriched in less polymerized melts [20,21] (i.e., on the right-hand side of the rhyolite–rhyolite couple shown in Fig 1). However, in the starting materials CaO is slightly enriched on the left-hand side. Therefore, the activity gradient for CaO is likely to be in the opposite direction to the concentration gradient and relatively large compared to the concentration gradient. Since CaO tries to maintain a transient 'equilibrium' partition, diffusion tends to

bring the concentration up on the right-hand side and down on the left-hand side. The uphill diffusion profile of CaO is qualitatively consistent with this idea. For K_2O in the rhyolite–rhyolite couple, two-liquid partition data suggest that at transient 'equilibrium' K_2O would be slightly enriched on the left-hand side (Fig. 1). Initially K_2O is strongly enriched (almost a factor of 2) on the right-hand side. Therefore, in this case the activity gradient of K_2O is likely to be in the same direction as the concentration gradient but just slightly different in absolute value. It is expected that there will be no uphill diffusion, consistent with our data. Upon closer inspection, the activity gradient is expected to be slightly greater than the concentration gradient and the EBD is expected to be slightly greater than the IEBD (see fig. 3B in [1]), again consistent with our data.

For FeO and K_2O in the rhyolite–andesite couple (Fig. 1), two-liquid partition data suggest that at transient 'equilibrium' FeO would be enriched in the less polymerized andesitic melt and K_2O in the more polymerized rhyolitic melt. Since initially FeO is already enriched in the andesitic melt and K_2O in the rhyolitic melt, exact values of pertinent two-liquid partition data are necessary to predict whether uphill diffusion occurs. If the initial enrichment is just right, the diffusion of the component would mimic that of SiO_2 and Al_2O_3. If the initial enrichment is insufficient, uphill diffusion will occur. If the initial enrichment is more than enough, uphill diffusion will not occur. The rough quantification of the two-liquid partition data in fig. 10 of [1] permits a prediction. It turns out that in both cases of FeO and K_2O the initial distributions are close to 'equilibrium' partition and a more precise knowledge of the partition coefficients than that provided by the rough quantification is necessary to predict the occurrence or absence of uphill diffusion.

As shown above, the transient 'equilibrium' partition concept as applied to diffusion is useful for a qualitative explanation of the features of the diffusion profiles. We now apply the modified effective binary diffusion model [1] (which is a quantification of the transient equilibrium concept) to fit the FeO, CaO and K_2O concentration profiles. The experimental concentration profiles are fit to the numerical solution of Eq. (6) in which γ is given by Eq. (7). For the CaO and K_2O profiles, the IEBD ($\mathfrak{D}$) is fixed to be that obtained from the respective isotopic fraction profile. Therefore only one parameter, Q, in Eq. (7) is adjustable in the fits. For the uphill diffusion profile of FeO in the rhyolite–andesite couple, both $\mathfrak{D}$ and Q are adjusted to optimize the fit. All the fits are good and three of them are shown in Fig. 4. The FeO profile in Fig. 4 is not perfectly fit near the two extreme points, suggesting variations in $\mathfrak{D}$ with composition. Values of two-liquid partition coefficient K calculated from the fitting parameter Q are comparable to those in [1]. The good fits show that in the context of the modified effective binary diffusion model the different lengths of the isotopic and concentration profiles and the uphill diffusion profiles can all be quantitatively explained. The uphill diffusion profile of CaO is consistent with its IEBD obtained from its isotopic fraction profile and can be modeled quantitatively. Likewise, the uphill diffusion profile of FeO can be explained quantitatively. The very short K_2O concentration profile (compared to its isotopic profile) in the andesite–rhyolite couple is consistent with the high IEBD of K_2O obtained from the isotopic profile and is caused by the absence of an activity gradient (note the flat activity profile in the bottom panel of Fig. 4). The absence of the activity gradient is due to the (unintentional) choice of an initial composition that was almost at transient 'equilibrium partitioning'. As a result, the diffusion profile mimics the SiO_2 profile in the experiment.

In conclusion, K_2O in the rhyolite–rhyolite couple shows no uphill diffusion and $D_K \approx \mathfrak{D}_K \gg D_{Si}$ because the K_2O concentration gradient is large and similar to its activity gradient. The K_2O in the rhyolite–andesite couple shows no uphill diffusion but $D_K \approx D_{Si} \ll \mathfrak{D}_K$ because the activity gradient is very small. CaO in the rhyolite–rhyolite couple shows uphill diffusion because the initial concentration difference between the two halves is small but the activity difference is large; CaO in the rhyolite–andesite couple shows $D_{Ca} < \mathfrak{D}_{Ca}$ and does not show up-

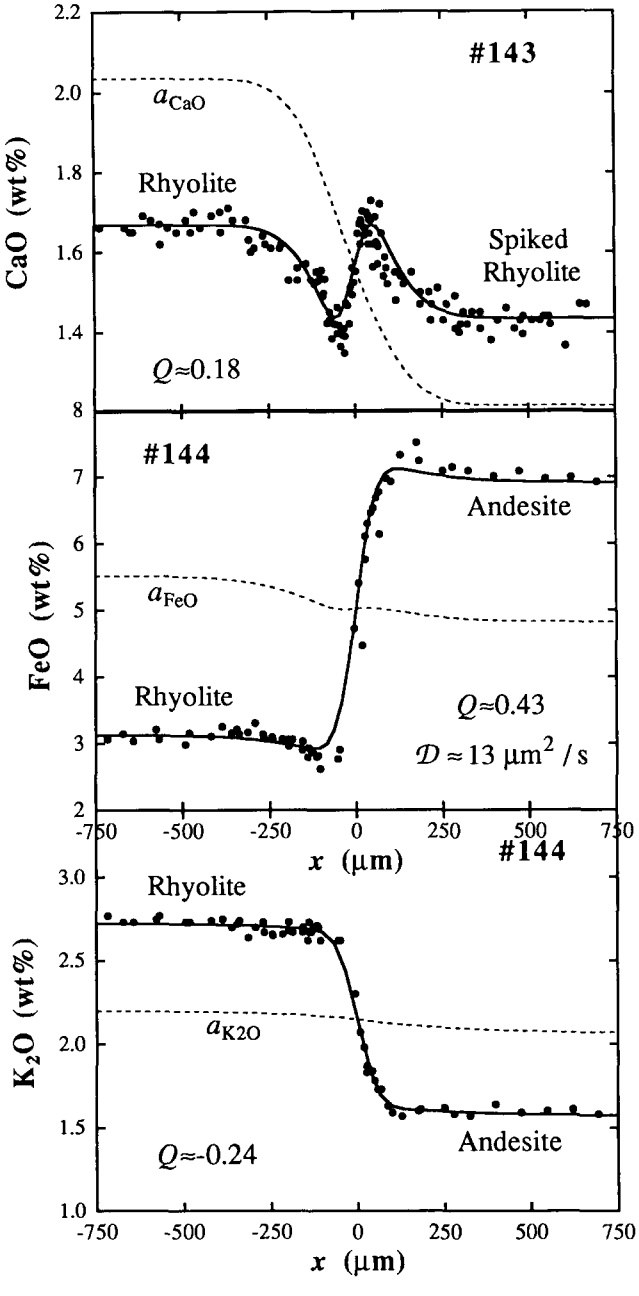

Fig. 4. Concentration profiles fit by the modified effective binary diffusion model [1]. Dots are electron microprobe data. Solid curves are best fits to the data and dashed curves are activity profiles calculated from fitting results.

hill diffusion because its activity gradient is smaller than the concentration gradient.

The above observations can be generalized as follows: When the activity gradient is similar to the concentration gradient (K_2O in the rhyolite–rhyolite couple), the EBD approaches the IEBD and the length of the concentration profile is similar to that of the isotopic fraction profile (i.e., homogenization of elemental and oxide concentration gradients is coupled with that of isotopic gradients). If the activity gradient is large and the concentration gradient small (CaO in the rhyolite–rhyolite couple) or if the activity gradient is in the opposite direction to the concentration gradient (FeO in the rhyolite–andesite couple), uphill diffusion occurs. If the activity gradient is small and the concentration gradient large (CaO and K_2O in the rhyolite–andesite couple), the EBD may be much smaller than the IEBD and the length of the concentration profile may be much shorter than that of the isotopic profiles (i.e., homogenization of elemental and oxide concentration gradients may be decoupled from isotopic gradients). All of our observations are quantitatively described by the modified effective binary diffusion model. Therefore, the multicomponent effects relevant to diffusion in our experiments seem to be largely due to the contribution of non-ideal mixing to the cross-terms of the D-matrix.

Acknowledgements

SvdL thanks the Hawaii Institute of Geophysics/SOEST for a fellowship. We thank D.R. Baker, J.N. Christensen, E.J. Essene, H.N. Pollack, F.J. Ryerson, F.J. Spera and an anonymous reviewer for their helpful comments. This research was supported by the US National Science Foundation (EAR-89-04375, EAR-89-16707 and EAR-93-04161) and by NASA (NAGW-1472 and NAG-9-43).

References

[1] Y. Zhang, A modified effective binary diffusion model, J. Geophys. Res. 98, 11901–11920, 1993.

[2] A.F. Trial and F.J. Spera, Measuring the multicomponent diffusion matrix: Experimental design and data

analysis for silicate melts, Geochim. Cosmochim. Acta, in press.
[3] A.R. Cooper, The use and limitations of the concept of an effective binary diffusion coefficient for multicomponent diffusion, in: Mass Transport in Oxides, J.B. Wachman and A.D. Franklin, ed., Natl. Bur. Std. Spec. Publ., pp. 79–84, 1968.
[4] A.W. Hofmann, Diffusion in natural silicate melts: a critical review, in: Physics of Magmatic Processes, R.B. Hargraves, ed., pp. 385–417, Princeton University Press, 1980.
[5] E.B. Watson and D.R. Baker, Chemical diffusion in magmas: an overview of experimental results and geochemical implications, in: Advances in Physical Geochemistry, 6, I. Kushiro and L. Perchuk, eds., pp. 120–151, Springer, 1991.
[6] Y. Zhang, D. Walker and C.E. Lesher, Diffusive crystal dissolution, Contrib. Mineral. Petrol. 102, 492–513, 1989.
[7] C.E. Lesher, Decoupling of chemical and isotopic exchange during magma mixing, Nature 344, 235–237, 1990.
[8] D.R. Baker, Tracer vs. trace element diffusion: diffusional decoupling of Sr concentration from Sr isotope composition, Geochim. Cosmochim. Acta 53, 3015–3023, 1989.
[9] L. Onsager, Theories and problems of liquid diffusion, Ann. N.Y. Acad. Sci. 46, 241–265, 1945.
[10] J.S. Kirkaldy and D.J. Young, Diffusion in the Condensed State, 527 pp., Inst. Metals, London, 1987.
[11] E.B. Watson, Basalt contamination by continental crust: some experiments and models, Contrib. Mineral. Petrol. 80, 73–87, 1982.
[12] F.J. Spera and A.F. Trial, Verification of Onsager's reciprocal relations in a molten silicate solution, Science 259, 204–206, 1993.
[13] F.M. Richter, A model for determining activity–composition relations using chemical diffusion in silicate melts, Geochim. Cosmochim. Acta 57, 2019–2032, 1993.
[14] A.D. Edgar, Experimental Petrology: Basic Principles and Techniques, 217 pp., Clarendon, Oxford, 1973.
[15] P.G. Shewmon, Diffusion in Solids, 203 pp., McGraw-Hill, New York, 1963.
[16] A.A. Clifford, Multivariate Error Analysis, 112 pp., Wiley, New York, 1973.
[17] A. Jambon, Tracer diffusion in granitic melts: Experimental results for Na, Rb, Cs, Ca, Sr, Ba, Ce, Eu to 1300°C and a model of calculation, J. Geophys. Res. 87, 10797–10810, 1982.
[18] E.B. Watson, Diffusion in magmas at depth in the earth: The effects of pressure and dissolved H_2O, Earth Planet. Sci. Lett. 52, 291–301, 1981.
[19] A.W. Hofmann and M. Magaritz, Diffusion of Ca, Sr, Ba, and Co in a basaltic melt: implications for the geochemistry of the mantle, J. Geophys. Res. 82, 5432–5440, 1977.
[20] E.B. Watson, Two-liquid partition coefficients: experimental data and geochemical implications, Contrib. Mineral. Petrol. 56, 119–134, 1976.
[21] F.J. Ryerson and P.C. Hess, Implications of liquid–liquid distribution coefficients to mineral–liquid partitioning, Geochim. Cosmochim. Acta 42, 921–932, 1978.
[22] S. Newman, E.M. Stolper and S. Epstein, Measurement of water in rhyolitic glasses: calibration of an infrared spectroscopic technique, Am. Mineral. 71, 1527–1541, 1986.